




Phosphorylation of JIP4 at S730 Presents Antiviral Properties against Influenza A Virus Infection

Juliana Del Sarto,^{a,b,c} Vanessa Gerlt,^a Marcel Edgar Friedrich,^a Darisuren Anhlan,^a Viktor Wixler,^a Mauro Martins Teixeira,^{b,c}
 Yvonne Boergeling,^a  Stephan Ludwig^a

^aInstitute of Virology Muenster, University of Muenster, Muenster, Germany

^bDepartment of Biochemistry and Immunology, Institute of Biological Sciences, Federal University of Minas Gerais, Belo Horizonte, Minas Gerais, Brazil

^cResearch Center for Drug Development, Institute of Biological Sciences, Federal University of Minas Gerais, Belo Horizonte, Minas Gerais, Brazil

Juliana Del Sarto and Vanessa Gerlt contributed equally to this work. Author order was determined alphabetically.

Yvonne Boergeling and Stephan Ludwig shared senior authorship.

ABSTRACT Influenza A virus (IAV) is the causative agent of flu disease that results in annual epidemics and occasional pandemics. IAV alters several signaling pathways of the cellular host response in order to promote its replication. Therefore, some of these pathways can serve as targets for novel antiviral agents. Here, we show that c-Jun NH₂-terminal kinase (JNK)-interacting protein 4 (JIP4) is dynamically phosphorylated in IAV infection. The lack of JIP4 resulted in higher virus titers, with significant differences in viral protein and mRNA accumulation as early as within the first replication cycle. In accordance, decreased IAV titers and protein accumulation were observed during the overexpression of JIP4. Strikingly, the antiviral function of JIP4 does not originate from modulation of JNK or p38 mitogen-activated protein kinase (MAPK) pathways or from altered expression of interferons or interferon-stimulated genes but rather originates from a direct reduction of viral polymerase activity. Furthermore, the interference of JIP4 with IAV replication seems to be linked to the phosphorylation of the serine at position 730 that is sufficient to impede the viral polymerase. Collectively, we provide evidence that JIP4, a host protein modulated in IAV infection, exhibits antiviral properties that are dynamically controlled by its phosphorylation at S730.

IMPORTANCE Influenza A virus (IAV) infection is a world health concern, and current treatment options encounter high rates of resistance. Our group investigates host pathways modified in IAV infection as promising new targets. The host protein JIP4 is dynamically phosphorylated in IAV infection. JIP4 absence resulted in higher virus titers and viral protein and mRNA accumulation within the first replication cycle. Accordingly, decreased IAV titers and protein accumulation were observed during JIP4 overexpression. Strikingly, the antiviral function of JIP4 does not originate from modulation of JNK or p38 MAPK pathways or from altered expression of interferons or interferon-stimulated genes but rather originates from a reduction in viral polymerase activity. The interference of JIP4 with IAV replication is linked to the phosphorylation of serine 730. We provide evidence that JIP4, a host protein modulated in IAV infection, exhibits antiviral properties that are dynamically controlled by its phosphorylation at S730.

KEYWORDS influenza virus, JIP4, host pathway, protein phosphorylation

Influenza A virus (IAV) is a common respiratory pathogen that infects up to 10% of the global population annually. IAV shows high mutation rates that lead to constant antigenic drift. Furthermore, there is a permanent threat of reassortment, potentially

Citation Del Sarto J, Gerlt V, Friedrich ME, Anhlan D, Wixler V, Teixeira MM, Boergeling Y, Ludwig S. 2021. Phosphorylation of JIP4 at S730 presents antiviral properties against influenza A virus infection. *J Virol* 95:e00672-21. <https://doi.org/10.1128/JVI.00672-21>.

Editor Bryan R. G. Williams, Hudson Institute of Medical Research

Copyright © 2021 American Society for Microbiology. All Rights Reserved.

Address correspondence to Stephan Ludwig, ludwigs@uni-muenster.de.

Received 20 April 2021

Accepted 27 July 2021

Accepted manuscript posted online

28 July 2021

Published 27 September 2021

leading to the generation of new highly pathogenic strains (antigenic shift). As a result, vaccines have to be annually updated according to predictions of circulating strains for the next epidemic season. Additionally, antiviral drugs that target IAV proteins present limited long-term efficacy due to increased viral resistance. Most of the FDA-approved IAV antivirals used in clinics today act as neuraminidase inhibitors (zanamivir, oseltamivir, and peramivir) or M2 channel blockers (adamantanes), all targeting specific viral proteins (1). Unfortunately, high rates of resistance against these drugs have been documented. Important examples are the global spread of oseltamivir-resistant seasonal influenza A (H1N1) viruses in 2007 and adamantane-resistant pandemic influenza A (H1N1) viruses in 2009 (2). As a strategy to avoid viral resistance, we aim to interfere with host cell proteins and pathways, posing less pressure for the development of viral escape variants.

During viral infection, the activity of several host cell signaling pathways is upregulated. While this can be primarily seen as a defense response of the infected cell, viruses have acquired the ability to misuse some of these pathways for their own purpose. Different pathways have already been shown to act in a virus-supportive manner, such as the Raf/MEK/extracellular signal-regulated kinase (ERK) cascade that modulates the export of viral ribonucleoproteins (vRNPs) from the nucleus into the cytoplasm in the later stages of the IAV replication cycle (3). Interestingly, another member of the family of mitogen-activated protein kinases (MAPKs), the c-Jun NH₂-terminal kinase (JNK), also showed virus-supportive activities (4), although it has been implicated in the regulation of the transcription factor activator protein 1 (AP-1) that is needed for efficient host antiviral responses (5). Likewise, the activation of MAPK p38 could be directly linked to the expression of interferon (IFN) and proinflammatory cytokines as well as to the modulation of IFN-induced responses (6). Different proteins have been reported to regulate or to be regulated by the pathways mentioned above, including a newly discovered protein named JNK-interacting protein 4 (JIP4) (7).

Besides the three similar proteins JIP1, JIP2, and JIP3, JIP4 belongs to the group of JNK-interacting proteins. All proteins of this group are known scaffold proteins that can interact with JNK and kinesin light chain (7). JIP4, also known as sperm-associated antigen 9 (SPAG9) or JNK-associated leucine zipper protein (JLP), is the most recently discovered protein of the JIP group, resulting in still little knowledge about its functions. Limited numbers of studies have been published identifying different activities of JIP4 in different scenarios. One showed that JIP4 phosphorylation is important during the G₂ phase of mitosis by its interaction with p38 MAPK (8). JIP4 has also been correlated with the promotion of an invasive phenotype of breast cancer cells through its interaction with proteins important for endosome tubulation and exocytosis (9). Despite the close relationship of JIP4 to JNK and p38 MAPKs, no functional association between JIP4 and virus infection has been described so far.

Therefore, we aimed to understand the role of JIP4 in IAV infection. In this study, we report antiviral properties of JIP4 against IAV *in vitro*. JIP4 phosphorylation at S730 interferes with viral polymerase activity, resulting in decreased viral replication. Hence, JIP4 represents a potential host target for therapeutic approaches.

RESULTS

JIP4 presents antiviral activity against IAV infection. Influenza virus replication leads to the regulation of several host pathways for both viral benefits and host-protective antiviral responses. Different host proteins have been shown to act in tightly organized networks to assist in the activation or inactivation of specific pathways. JIP4 has been shown not only to bind but also to interfere with the activation of the MAPKs JNK and p38, two proteins highly reported to present relevant functions in IAV infection (7). In order to investigate the possible role of JIP4 in IAV infection, we transfected A549 cells with small interfering RNAs (siRNAs) specifically targeting JIP4 and analyzed the replication efficiency of IAV H1N1 A/Puerto Rico/8/34 (PR8). Viral titers were increased in JIP4-silenced cells, and this effect was maintained over multiple replication cycles, resulting in

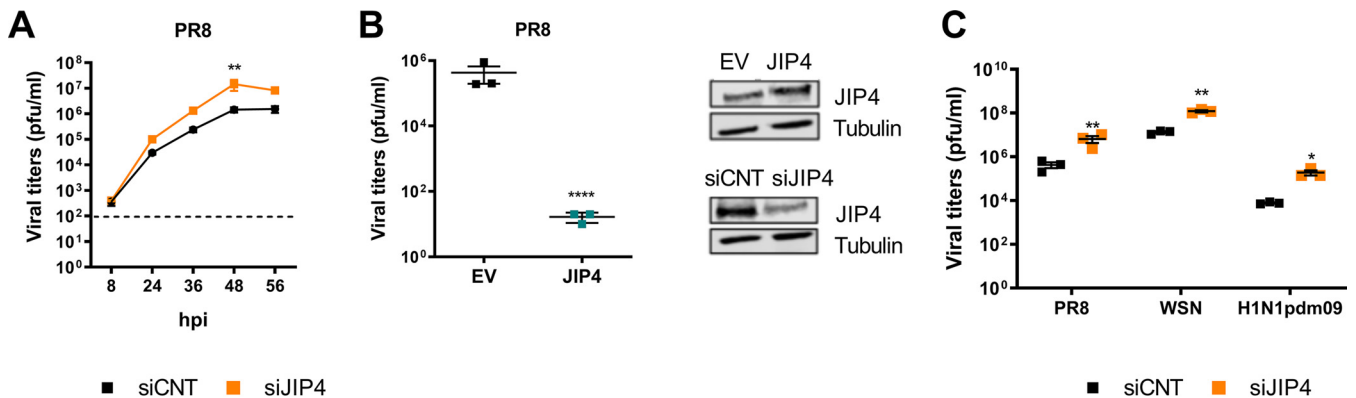


FIG 1 JIP4 presents antiviral activity against IAV infection. (A) A549 cells were transfected with siRNAs targeting JIP4 (siJIP4) or control siRNA (siCNT) 2 days prior to infection. Cells were then infected with PR8 IAV (MOI of 0.1). Supernatants were collected at 8, 24, 36, 48, and 56 hpi and analyzed for viral titers by standard plaque assays. Cells were collected for evaluation of the knockdown efficiency via Western blotting; tubulin detection served as a loading control. Results were statistically analyzed by two-way analysis of variance (ANOVA). (B) A549 cells were transfected with either an empty vector (EV) or plasmids containing the JIP4 sequence and infected with PR8 (MOI of 0.1). Supernatants were collected at 48 hpi for analysis of viral titers by standard plaque assays. Cells were collected for evaluation of the overexpression efficiency by Western blotting; tubulin detection served as a loading control. Results were statistically analyzed by a *t* test. (C) A549 cells were transfected with siJIP4 or siCNT and infected with different IAV strains 2 days post-transfection. PR8, WSN, or H1N1pdm09 was administered at an MOI of 0.1. Supernatants were collected at 48 hpi for determination of viral replication abilities by standard plaque assays. Results were analyzed by independent *t* tests per strain. *, $P < 0.05$; **, $P < 0.01$; ****, $P < 0.0001$ (compared to the respective controls). All Western blot images are representative of results from three independent experiments. Graphs are a compilation of results from three independent experiments.

significant differences at 48 h post-infection (hpi) (Fig. 1A). In agreement, the overexpression of JIP4 resulted in a strong reduction in virus replication (Fig. 1B). Cells from the respective experiments were analyzed by Western blotting to confirm the silencing or overexpression of JIP4. Similar to PR8, A/WSN/33 (WSN) and the clinically relevant A/Hamburg/04/09 (H1N1pdm09) strain also presented higher replication rates in JIP4-silenced cells than in control cells (Fig. 1C). Overall, these results suggest an antiviral function of JIP4 in IAV infections.

JIP4 interferes with IAV replication prior to viral protein expression. We next examined at which step of the IAV life cycle JIP4 would restrict virus replication. Therefore, JIP4-silenced A549 cells were infected with PR8 at a multiplicity of infection (MOI) of 5, and the expression of viral proteins was analyzed by Western blotting (Fig. 2A). Interestingly, the expression levels of viral nonstructural protein 1 (NS1) and polymerase basic protein 1 (PB1), which were chosen as representatives of early and late viral proteins, respectively, were increased in the absence of JIP4 compared to the control. To further confirm this phenotype, we evaluated viral protein amounts after the overexpression of JIP4. Accordingly, viral protein expression was highly decreased in JIP4-overexpressing cells compared to empty vector (EV)-transfected cells (Fig. 2B). Therefore, we conclude that JIP4 possesses an antiviral activity already in the early stages of viral replication, altering the production of viral proteins.

We next analyzed if the differences observed in viral protein expression are a consequence of alterations in translation or transcription steps by performing quantitative real-time PCR (qRT-PCR) analysis of viral mRNAs of PB1, NS, and matrix protein 1 (M1) (Fig. 2C). Interestingly, all viral mRNAs analyzed presented increased expression levels in JIP4-silenced cells compared to control cells. The silencing efficiency was confirmed by the detection of low copy numbers of SPAG9 mRNA.

Overall, these results demonstrate that the antiviral function of JIP4 is effective in the early stages of viral replication, resulting in altered viral mRNA levels and, consequently, viral protein expression, finally leading to decreased virus titers.

The antiviral function of JIP4 does not correlate with MAPK JNK- or p38-induced antiviral responses. Throughout IAV infection, host cells produce IFNs to induce an antiviral state, which is mainly orchestrated by IFN beta (IFN- β) (10). The presence of IFNs launches the expression of IFN-stimulated genes (ISGs) in neighboring cells, which are subsequently protected from potential infection. The induction of IFN- β expression

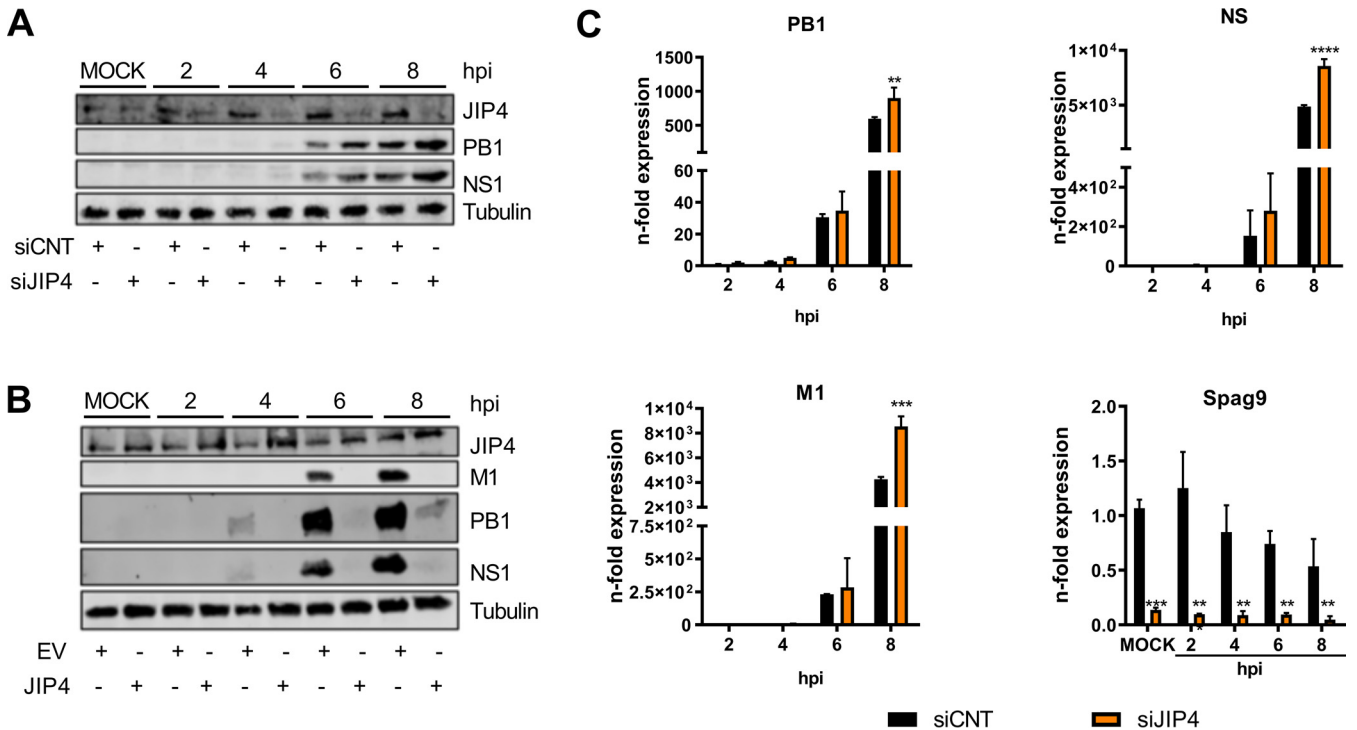


FIG 2 JIP4 interferes with IAV replication prior to viral protein expression. (A) A549 cells were transfected with either control siRNA (siCNT) or siRNAs targeting JIP4 (siJIP4) and infected with PR8 (MOI of 5). Cells were lysed every 2 h. Lysates were submitted to Western blot assay and incubated with antibodies against the viral proteins PB1 and NS1 as well as against JIP4 for silencing confirmation. Detection of tubulin served as a loading control. + and – indicate the presence and absence, respectively, of the respective siRNAs. (B) A549 cells were transfected with either an empty vector (EV) or plasmids encoding JIP4 and infected with PR8 (MOI of 5). + and – indicate the presence and absence, respectively, of the respective plasmids. Cells were lysed every 2 h. Lysates were submitted to Western blot assays and incubated with antibodies against the viral proteins PB1, NS1, and M1 as well as against JIP4 for overexpression confirmation. Detection of tubulin was used as a loading control. (C) For analyses of viral mRNA expression, A549 cells were transfected with either siCNT or siJIP4 and infected with PR8 (MOI of 5). Samples were collected every 2 h and processed for qRT-PCR analyses. Viral mRNAs were normalized to the 2 h control group. *SPAG9* gene expression was normalized to the mock control. Results were statistically analyzed by two-way ANOVA. **, $P < 0.01$; ***, $P < 0.001$; ****, $P < 0.0001$ (compared to the respective controls). All Western blot images are representative of results from three independent experiments. Graphs are a compilation of results from three different experiments.

is a result of the activation of different signaling cascades within the cell (11). Especially, our group has shown that the activation of the MAPKs p38 and JNK is required for type I IFN production in IAV infection (5, 6). Since JIP4 has been shown to bind to both JNK and p38 MAPKs (7), we were prompted to evaluate if the antiviral activity could be linked to a modulation of IFN- β production. For that, A549 cells transfected with control or JIP4-targeting siRNAs were infected with PR8 and analyzed for IFN- β and ISG expression by qRT-PCR. In control cells, the steadily increasing induction of IFN- β at a low level correlated well with the continuous increase in the expression of the downstream ISGs MxA and IP10 upon infection (Fig. 3A). Interestingly, the absence of JIP4 did not significantly alter the expression of these genes.

MAPK p38 has been shown to act not only in type I IFN production but also in IFN-mediated cell signaling (6). Therefore, we next evaluated if the absence of JIP4 would result in alterations in IFN signaling in a virus replication-independent approach. For that, cells were transfected with siRNAs targeting JIP4 and stimulated with recombinant IFN- β . qRT-PCR was used for the quantification of ISG expression. MxA as well as OAS1 were induced upon stimulation; nevertheless, no differences in expression levels were observed between control and JIP4-silenced cells (Fig. 3B).

These results suggest that there is no involvement of IFN expression or responses in the antiviral activity of JIP4 in influenza A virus infection. In order to further confirm this hypothesis, we transfected cells with siRNAs targeting JIP4 and infected them with vesicular stomatitis virus (VSV) at an MOI of 0.1, which has been shown to be highly sensitive to IFN responses (12). As expected, the absence of JIP4 did not alter VSV replication (Fig. 3C). To further confirm that the lack of effects is not due to saturated VSV

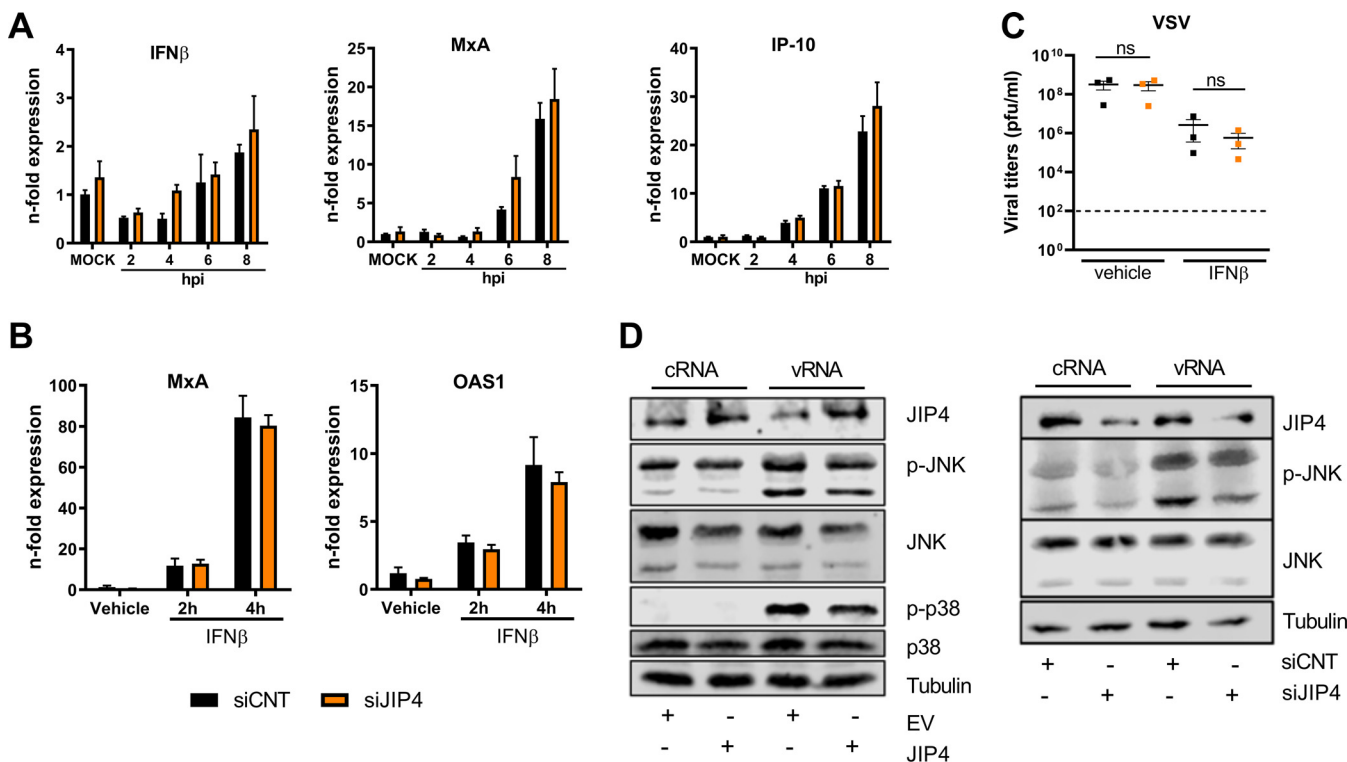


FIG 3 The antiviral role of JIP4 does not correlate with changes in IFN responses or JNK/p38 activation. (A) A549 cells were transfected with either control siRNA (siCNT) or siRNAs targeting JIP4 (siJIP4) and infected with PR8 (MOI of 5). Cells were collected every 2 h for qRT-PCR analysis focusing on IFN and ISG mRNA expression. Results were statistically analyzed by two-way ANOVA. (B) A549 cells were transfected with either siCNT or siJIP4 and stimulated with IFN- β for 2 or 4 h. ISG mRNA levels were analyzed by qRT-PCR. Results were statistically analyzed by two-way ANOVA. Results in panels A and B are depicted as *n*-fold expression over mock/vehicle after normalization to GAPDH expression. (C) A549 cells were transfected with either siCNT or siJIP4, infected with VSV (MOI of 0.01), and treated with the vehicle or 100 U IFN- β . Supernatants were collected at 24 hpi, and virus replication was analyzed by standard plaque assays. Results are expressed as PFU per milliliter and were statistically analyzed by a *t* test. ns, not significant. (D) For analysis of JNK and p38 activity, A549 cells were transfected with either EV or JIP4-expressing plasmids (left) or siRNAs (right) and incubated for 24 h. Cells were then further transfected with cRNAs/vRNAs to stimulate the activation of JNK and p38 kinases. After 3 h of stimulation, cells were lysed for Western blot analysis, and the activation of MAPKs was determined by using p-JNK and p-p38 antibodies. Detection of p38, JNK, and tubulin served as loading controls; successful overexpression or knockdown was confirmed by JIP4 detection. All Western blot images are representative of results from three independent experiments. + and - indicate the presence and absence, respectively, of the respective siRNAs or plasmids. Graphs are a compilation of results from two independent experiments.

replication, silenced cells were treated with 100 U of IFN- β directly after VSV infection. As observed previously, there were no differences between control siRNA-transfected and JIP4-depleted cells, clearly indicating that JIP4 does not function as a modulator of the type I IFN response.

Finally, since type I IFN production or signaling was not altered in the absence of JIP4, we analyzed whether the protein would affect the IAV-induced activation of the kinases JNK and p38. For that, JIP4-overexpressing cells were stimulated with total RNA collected from either mock-infected (control RNA [cRNA]) or IAV-infected (viral RNA [vRNA]) cells and analyzed for the activation of the MAPKs JNK and p38. In this assay, the vRNA pool isolated from infected cells served as a pathogen-associated molecular pattern (PAMP) to stimulate p38 and JNK activity. Our results clearly demonstrate that the overexpression of JIP4 does not significantly alter JNK or p38 activation after vRNA stimulation, even though both kinases showed a slight reduction in phosphorylation, which can most likely be attributed to marginally decreased amounts of total protein after JIP4 overexpression (Fig. 3D). Similar results were observed after siRNA-mediated knockdown of JIP4. Here, the absence of the protein did not significantly alter JNK phosphorylation compared to the activation observed in control siRNA-transfected cells.

Altogether, the antiviral role of JIP4 is correlated with neither an altered activation of JNK or p38 MAPKs nor higher IFN- β responses.

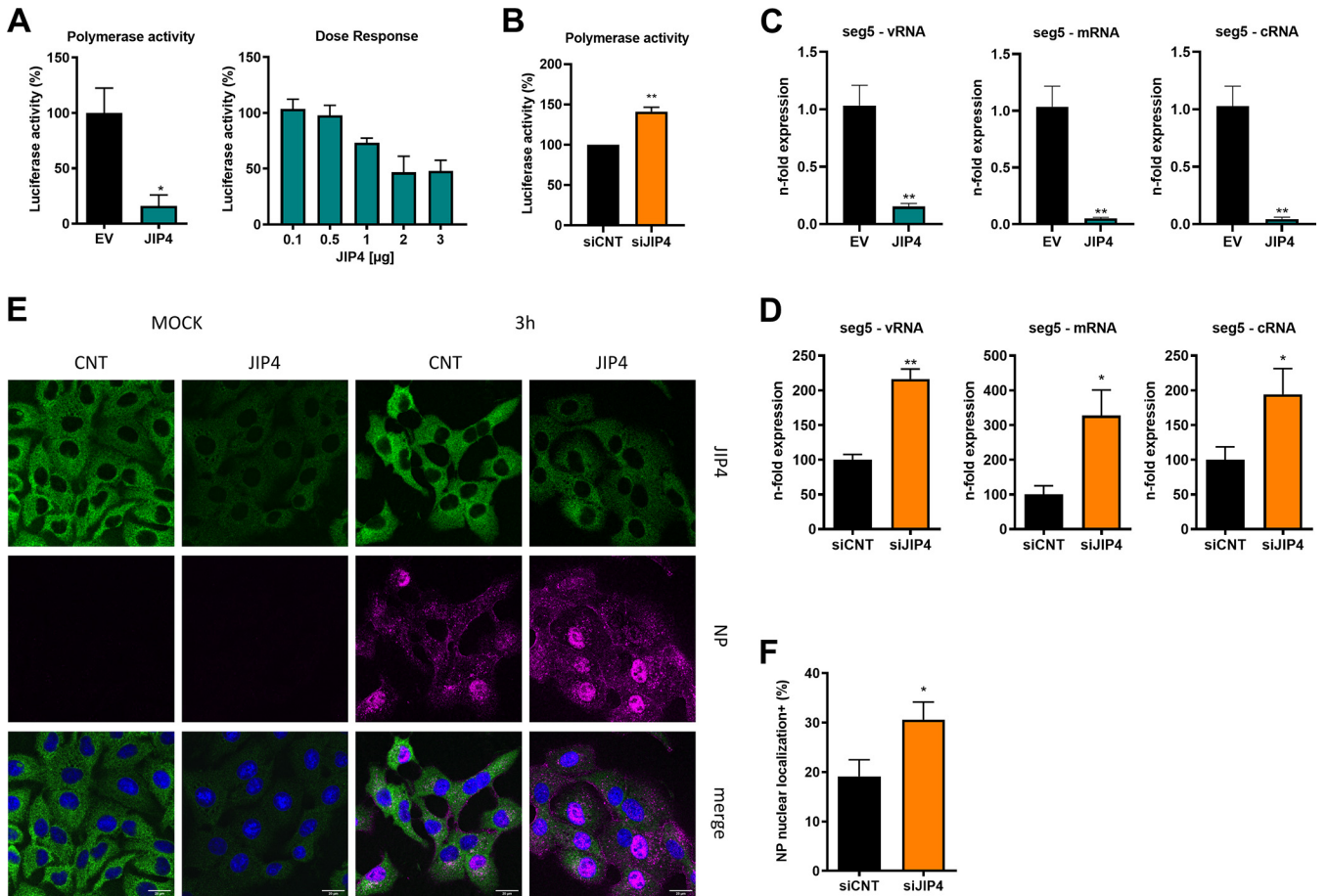


FIG 4 JIP4 overexpression decreases viral polymerase activity. (A) Vero cells were transfected with either an empty vector (EV) or JIP4-expressing plasmids together with all viral polymerase subunits and a reporter gene. At 24 hpt, cells were collected for luciferase assays. The activity in EV-transfected cells was arbitrarily set to 100%. For dose-response determinations, luciferase activities measured in JIP4-transfected cells are presented as percentages over the respective GST-expressing controls. (B) Vero cells were transfected with either control siRNA (siCNT) or siRNAs targeting JIP4 (siJIP4). At 48 hpt, cells were transfected with all viral polymerase subunits and a reporter gene. Twenty-four hours after the second transfection, cells were collected for luciferase assays. The activity in siCNT-transfected cells was arbitrarily set to 100%. (C) A549 cells were transfected with either EV or JIP4-expressing plasmids for 24 h and infected with PR8 (MOI of 5). Total RNA was collected at 4 hpi for strand-specific qRT-PCR. (D) A549 cells were transfected with either siCNT or siJIP4 and infected with PR8 (MOI of 5). Total RNA was collected at 4 hpi for strand-specific qRT-PCR. (E) A549 cells were transfected with either control siRNA or siRNAs targeting JIP4. After 48 h of transfection, cells were infected with PR8 (MOI of 20) and collected for immunofluorescence assays at 3 hpi. The localization of JIP4 and NP was analyzed by using specific antibodies; nuclei were stained with DAPI. (F) Percentage of cells with nuclear NP localization expressed over the total number of cells in the field. **, $P < 0.01$; *, $P < 0.05$ (compared to the respective controls). Polymerase activity graphs are a compilation of results from three independent experiments. Strand-specific PCR graphs with overexpression represent data from one experiment with three replicates; JIP4 knockdown strand-specific PCR graphs are compilations of data from two independent experiments. The immunofluorescence image is representative of results from three independent experiments. All results mentioned above were statistically analyzed by a *t* test (Welch's *t* test [B]).

JIP4 interferes with viral polymerase activity. After receptor-mediated endocytosis of influenza virions and the release of the eight single-stranded viral RNA segments (vRNPs) into the cytoplasm (13), the trimeric viral RNA-dependent RNA polymerase, composed of the PB1, PB2, and polymerase acidic protein (PA) subunits, is responsible for the transcription and replication of the genomic segments (14). Since JIP4 altered the expression of viral mRNAs, we hypothesized that it might interfere with the machinery involved in viral RNA synthesis and, hence, the viral polymerase. To test this hypothesis, we performed a minigenome assay by transfecting cells with all subunits of the viral polymerase complex together with nucleoprotein (NP), an influenza-like luciferase reporter gene, and either JIP4-encoding or empty vector plasmids. Viral polymerase reconstitution assays were performed in type I IFN-deficient Vero cells in order to exclude any further interference of the type I IFN system. Indeed, JIP4-overexpressing cells showed a significant reduction in viral polymerase activity by approximately 75% compared to control cells (Fig. 4A). Furthermore, normalization to the polymerase activity measured in glutathione *S*-transferase (GST)-expressing cells uncovered

a dose-dependent polymerase-inhibiting effect of JIP4, which cannot be attributed to unspecific blocking of luciferase translation. To exclude that supraphysiological levels of JIP4 might inhibit expression from the helper plasmids expressing the viral polymerase subunits, the effects of siRNA-mediated knockdown of JIP4 were assessed (Fig. 4B). As expected, there was significantly increased viral polymerase activity observable, indicating a rather direct action of JIP4 in the regulation of viral polymerase function.

We further analyzed whether viral genome replication is also modulated by JIP4 via evaluating the expression of the three different RNA strands (vRNA, cRNA, and mRNA) of gene segment 5 (NP) at 4 hpi. Here, the overexpression of JIP4 resulted in significant decreases in the levels of all three RNA strands (Fig. 4C). Importantly, in the absence of JIP4, the expression of all three RNA strands was significantly increased (Fig. 4D), which can most likely be attributed to elevated expression of viral polymerase proteins already early in the replication cycle.

To understand whether JIP4 affects viral polymerase activity by a direct action on the polymerase complex in the nucleus, we analyzed the subcellular localization of JIP4 by immunofluorescence (Fig. 4E). As described previously (7), JIP4 is exclusively observed in the cytoplasm, even after infection. These results indicate that a direct interaction of JIP4 with the viral polymerase complex inside the nucleus is rather unlikely. However, cells transfected with siRNAs targeting JIP4 presented a significantly higher percentage of NP-positive nuclei early in the replication cycle than control cells (Fig. 4F).

Altogether, these results demonstrate that JIP4 possesses anti-IAV activity that seems to be independent of direct interference with viral polymerase complexes in the nucleus but might be related to a hijacking activity with respect to incoming vRNPs, PB1-PA complexes, PB2, or NP in the cytoplasm.

Phosphorylation of JIP4 at S730 seems to be a prerequisite for its antiviral function. Protein activities can be regulated by different mechanisms, including post-translational modifications such as phosphorylation or dephosphorylation. In order to analyze whether JIP4 function is modulated by dynamic phosphorylation in IAV infection, we performed a quantitative mass spectrometry analysis. A549 cells were infected with IAV strain PR8, A/FPV/79/Bratislava (H7N7) (FPV), or A/Thailand/KAN-1/2004 (H5N1) (KAN-1) at an MOI of 5, and the JIP4 phosphorylation status as well as protein amounts were analyzed at 0, 2, 4, 6, and 8 hpi. The respective phosphorylation intensities were normalized to JIP4 protein amounts and expressed as *n*-fold over noninfected cells. Here, we identified the tryptic JIP4 peptide SASQSSLDK (mass error of $1.34\text{E}-01$ ppm, with a posterior error probability [PEP] of $1.79\text{E}-20$) to be increasingly phosphorylated during viral life cycle progression at the third amino acid (S730) with a localization probability of 1 (Fig. 5A). This phosphorylation was already detectable as early as 2 h after infection with the PR8 and KAN-1 strains and further elevated after infection with all tested strains at 6 hpi (Fig. 5B). Next, we wanted to investigate if S730 phosphorylation is responsible for the antiviral activity of JIP4 in IAV infection. Therefore, we used plasmids containing mutations in the specific phosphosite changing the serine to nonphosphorylatable alanine (A) or glutamic acid (E), the latter mimicking a constitutively phosphorylated state, and analyzed IAV polymerase activity. As observed previously, the overexpression of wild-type (WT) JIP4 resulted in a significant reduction in viral polymerase activity. Interestingly, the presence of nonphosphorylatable JIP4 S730A rescued the activity observed in EV-transfected control cells. In contrast, JIP4 S730E reduced viral polymerase activity to a level similar to that observed for WT JIP4 (Fig. 5C). These results indicate a possible relationship between JIP4 S730 phosphorylation and the antiviral role of the protein in IAV infection.

DISCUSSION

IAV is a widespread respiratory pathogen that infects 10% of the global population annually. Antiviral treatments are urgently needed. Targeting host pathways is a promising approach to avoid the development of resistance. We have identified a novel antiviral function of the cellular JIP4 protein in IAV infection that is independent of

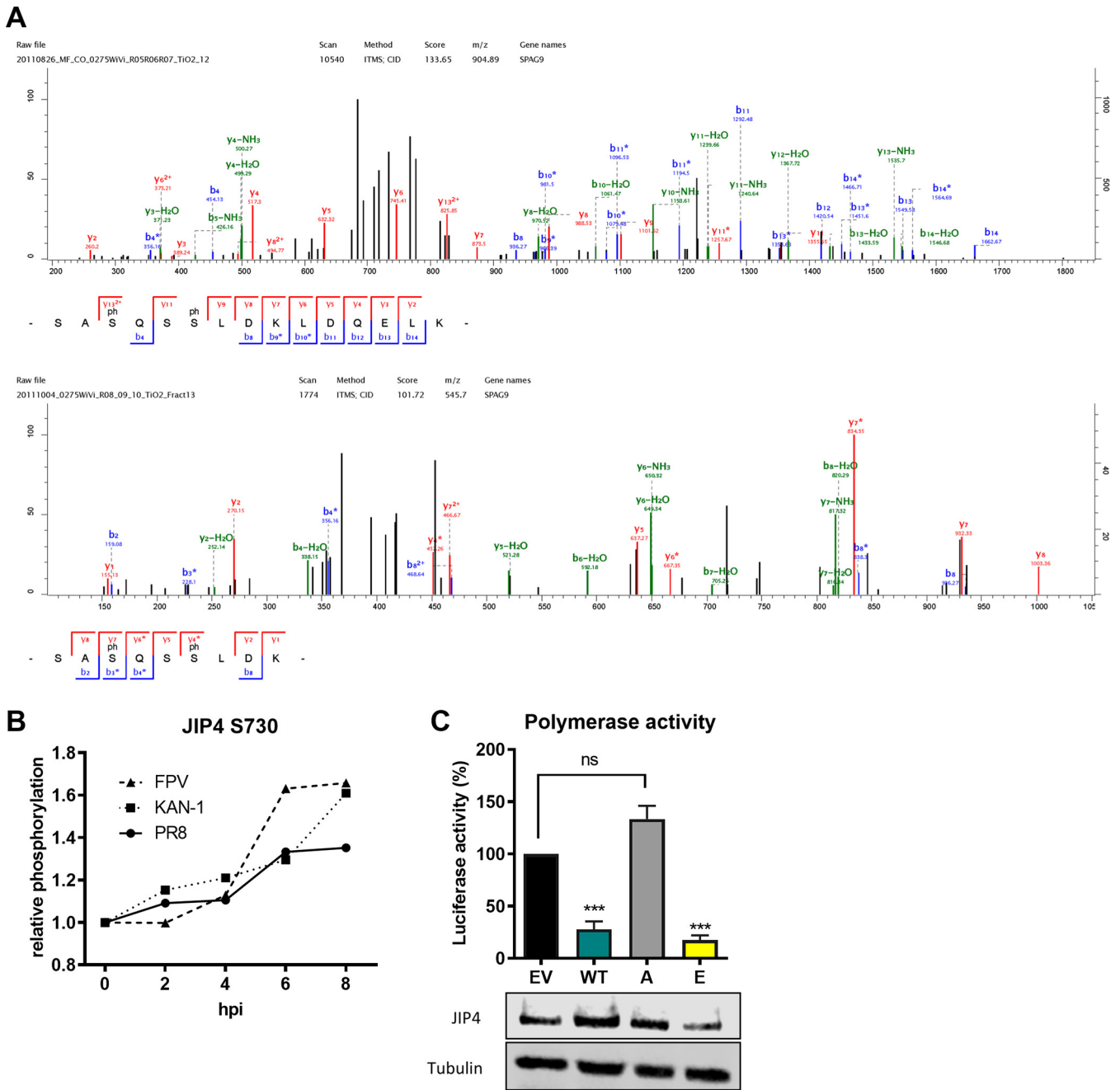


FIG 5 Phosphorylation of JIP4 S730 results in decreased viral polymerase activity. (A) A549 cells were labeled by using SILAC and infected with low-pathogenic IAV strain PR8 (H1N1) or one of two highly pathogenic strains (H5N1 strain KAN-1 and H7N7 strain FPV). Samples were collected at 2, 4, 6, and 8 hpi and analyzed for JIP4 phosphorylation. Representative MS/MS spectra of the tryptic peptides SASQSSLDKLDQELK (top) and SASQSSLDK (bottom) show phosphorylation at S730. ITMS, ion trap mass spectrometry; CID, collision-induced dissociation. (B) Relative phosphorylation of JIP4 at S730 at different time points compared to non-infected cells after normalization to the respective JIP4 protein amounts. (C) Vero cells were transfected with either EV or plasmids expressing WT JIP4 or the JIP4 phospho-mutant S730A or S730E together with all viral polymerase subunits and a reporter gene. At 24 hpt, cells were collected for luciferase assays. The activity in EV-transfected cells was arbitrarily set to 100%, and all groups were statistically compared with EV-transfected cells by one-way ANOVA. Overexpression was confirmed by Western blotting. ***, $P < 0.001$ (compared to the control group). Mass spectrometry phosphorylation kinetic data are the results from a single experiment. The polymerase activity graph is a compilation of data from three independent experiments.

type I IFN production or p38/JNK MAPK activation. JIP4 influences the IAV life cycle in the early stages of viral replication, resulting in decreased viral polymerase activity. Furthermore, we identified the phosphorylation of JIP4 at S730 to be decisive for its antiviral function.

Here, the lack of JIP4 resulted in higher viral replication of IAV. Our results also point

to an early effect on viral replication since we could already observe differences in viral mRNA and protein expression by as early as 4 hpi.

As already suggested by the name of the protein family, one of the well-known interaction partners of the JIP family is JNK since all members possess a JNK binding site (15). JNK activation has been observed after infection with several different viruses, and, particularly in IAV infection, the activation of JNK was shown to exhibit both virus-supportive and antiviral functions (16–18). Besides this common function of JIP family members, JIP4 has specifically been reported to also bind to p38 MAPK (8). The link between the p38 MAPK pathway and inflammation has been well established. Our group previously reported how p38 inhibition leads to protection against IAV *in vivo* due to its suppression of cytokine amplification. In addition, our group also showed the influence of p38 inhibition on the production of the main antiviral responses orchestrated by type I IFN, especially IFN- β (6). In accordance with the literature, JIP4 overexpression resulted in slight alterations of both phosphorylated and total amounts of JNK and p38. Nevertheless, the absence of JIP4 did not result in alterations in the production of IFN or ISGs. These results are in agreement with the literature that reported key differences of JIP4 compared to other proteins of the JNK-interacting protein group. The lack of an ability to bind to mitogen-activated protein (MAP) kinase kinase 7 (MKK7) and mixed-lineage kinase 3 (MLK3), two upstream proteins of the JNK signaling pathway, suggests that JIP4 might not act as a scaffold protein as previously characterized for the other members of the group (7). In this sense, we could exclude a modulation of p38 and JNK activation as an explanation for the observed antiviral activity of JIP4.

JIP4 absence resulted in lower viral mRNA levels, demonstrating interference with the viral life cycle prior to or during transcriptional steps. IAV polymerase activity showed a significant decrease upon JIP4 overexpression without an indication of direct interference with the viral polymerase complex in the nucleus. Since JIP4 is a recently discovered protein, little is known about its different roles in cell biology, especially during viral infections. Hence, it is still mechanistically unclear how JIP4 alters viral polymerase activity. JIP4 has previously been shown to interact with ARF6 (ADP-ribosylation factor 6) at the cell membrane, which was correlated with the control of the trafficking of recycling endosomes into and out of the intercellular bridge, together with the function in abscission during cell division (9). Furthermore, it was recently shown that JIP4 also interacts with leucine-rich repeat kinase 2 (LRRK2) orchestrating the formation of lysosome-associated membrane protein 1 (LAMP1)-negative tubules to release vesicles from lysosomes traveling through the cytosol and interacting with other lysosomes and possibly other cellular organelles as part of a new sorting mechanism (19). Nevertheless, our minigenome assay is performed with direct transfection of the polymerase complex subunits; thus, we can already exclude that JIP4 would alter viral entry and/or uncoating, both early steps in viral replication that depend on host cell membranes. The exact mechanism of how JIP4 interferes with IAV replication remains elusive, but we hypothesize that JIP4 interferes with the import of incoming vRNPs or distinct newly synthesized polymerase subunits into the nucleus. However, the possible involvement of JIP4 in viral protein translation that would also interfere with viral mRNA expression cannot be ruled out so far.

The antiviral activity of JIP4 seems to be correlated with S730 phosphorylation. Interestingly, it is well described that different kinases present important roles during IAV infection, and MAP kinases, especially the Raf/MEK/ERK pathway, have been previously reported to be involved in the regulation of JIP4 S730 phosphorylation (20, 21). It should be mentioned that, so far, we cannot fully exclude an influence of the introduced substitutions for serine rather than the missing/mimicked phosphorylation at S730 alone. However, site S730 has already been identified to be phosphorylated in different species, including humans, mice, and rats. Nevertheless, no specific role has been assigned to it yet. The importance of the virus-supportive role of the Raf/MEK/ERK signaling cascade in IAV infection is well documented (22–24). ERK signaling has been shown to be activated in different stages of the IAV life cycle, including the first

hours during viral entry and uncoating as well as a second activation during vRNP nuclear export (25, 26). Interestingly, previously described ERK activation dynamics nicely correlate with the observed JIP4 S730 phosphorylation kinetics since it seems to already be in a phosphorylated state at 2 hpi and further increased after 6 h of IAV infection. Our group has exceedingly shown that MEK inhibition results in an overall decrease of viral replication (22, 24), highlighting again how efficient viruses are in the misuse of cellular pathways that also provide antiviral functions, as observed previously for MAPK JNK or the NF- κ B pathway (4, 27, 28). Further unraveling of the detailed mechanism of the antiviral activity of JIP4 as well as the identification of the kinases involved in its phosphorylation might provide alternative ways to develop new antiviral approaches.

In summary, we have identified a novel antiviral function of the JIP4 protein in IAV infection. We showed that the virus-restricting function of JIP4 is not due to a modulation of JNK or p38 MAPK signaling cascades or alterations in IFN production or signaling. We have demonstrated that JIP4 seems to alter viral polymerase activity without a direct interaction with the vRNP complex in the nucleus. Furthermore, we have identified dynamic phosphorylation of JIP4 at S730 to be supposedly responsible for the observed antiviral function. We conclude that JIP4 might be a promising target for IAV antiviral therapy.

MATERIALS AND METHODS

Virus strains and cell lines. IAV H1N1 strains A/Puerto Rico/8/34, A/WSN/33, and A/Hamburg/04/09 were taken from virus collections of the Institute of Virology Muenster. A/Thailand/KAN-1/2004 (H5N1) was used with kind permission from P. Puthavathana (Bangkok, Thailand). A/FPV/79/Bratislava (H7N7) (fowl plague virus) was originally obtained from the Institute of Virology in Giessen, Germany. Influenza viruses as well as vesicular stomatitis virus (VSV) strain Indiana were propagated on Madin-Darby canine kidney II (MDCKII) cells cultured in minimal essential medium (MEM; Sigma) containing 10% (vol/vol) fetal calf serum (FCS; Biochrom). Human alveolar epithelial cells (A549) and green monkey epithelial cells (Vero) were cultured in Dulbecco's modified Eagle's medium (DMEM; Sigma) containing 10% FCS. All cell lines were originally purchased from the ATCC and have been passaged in the laboratory. At regular intervals, cells are checked for their identity by single nucleotide polymorphism (SNP) profiling (Multiplexion).

Reagents and plasmids. JIP4-expressing plasmids pRP-EGFP/Puro-CAG-JIP4 WT (wild type), -JIP4 S730A, and -JIP4 S730E were purchased from VectorBuilder. All constructs for the viral polymerase reconstitution assay were created as previously described (29). All plasmids were transformed into competent bacterial cells (*Escherichia coli* XL-Gold) and propagated in LB medium with 25 μ g/ml ampicillin, and plasmid purifications were performed according to the manufacturer's instructions (Sigma).

Recombinant human type I interferon (interferon beta [IFN- β]) was obtained from PBL Assay Science and added at a concentration of 100 U/ml to the medium of seeded A549 cells.

Mass spectrometry. For the measurement of JIP4 phosphorylation dynamics, stable isotope labeling by amino acids in cell culture (SILAC) was used. Human A549 cells stably labeled with either "light" lysine ($^{12}\text{C}_6$, $^{14}\text{N}_2$) and arginine ($^{12}\text{C}_6$, $^{14}\text{N}_4$), "medium" lysine ($^{13}\text{C}_6$, $^{14}\text{N}_2$) and arginine ($^{13}\text{C}_6$, $^{14}\text{N}_4$), or "heavy" lysine ($^{13}\text{C}_6$, $^{15}\text{N}_2$) and arginine ($^{13}\text{C}_6$, $^{15}\text{N}_4$) were infected with PR8, FPV, or KAN-1 (MOI=5) for 0, 2, 4, 6, and 8 h. Here, medium-labeled and heavy-labeled cells were infected for 2 or 6 h and 4 or 8 h, respectively, while light-labeled cells were always used as non-infected controls (0 h). Lysates from cells infected for 0, 2, and 4 h were mixed equally and used as the first sample, while equally mixed lysates from cells infected for 0, 6, and 8 h were used as the second sample. After tryptic digestion, samples were subjected to proteome analysis and a separate phosphoproteome analysis by cation-exchange chromatography with or without TiO_2 -based phosphopeptide enrichment chromatography, respectively, followed by liquid chromatography-tandem mass spectrometry (LC-MS/MS) analysis on a Proxeon Easy-nLC instrument coupled to an LTQ-Orbitrap XL mass spectrometer to discriminate between regulation at the P site and the protein level. Data were processed using Mascot and MaxQuant software (v1.2.2.9) as previously described (30, 31). Dynamics of the phosphorylation intensities of JIP4-derived peptides were quantified in relation to the ratio of total JIP4 protein expressed at the different time points analyzed, normalized to the intensities in non-infected cells.

Transfection and RNA stimulation. For JIP4 silencing, A549 or Vero cells were transfected in suspension with 50 pmol per 3×10^5 or 2.5×10^5 cells of scrambled siRNAs (control, 5'-UUCUCCGACGU GUCACGU-3') or siRNAs specific for JIP4 (5'-GAGCAUGUCUUACAGAUUU-3') using the transfection reagent Lipofectamine 2000 (Invitrogen) or TransIT-LT1 (Mirus) according to the manufacturer's instructions. Medium was exchanged at 24 h post-transfection (hpt), and infection was carried out for 48 h.

For the overexpression of WT JIP4 or JIP4 mutants, A549 or Vero cells were transfected with 3 μ g of plasmids with the transfection reagent Lipofectamine 2000 (Invitrogen) according to the manufacturer's instructions at 24 h post-seeding. Empty vector (EV) plasmids were used as transfection controls. Medium exchange was performed at 4 hpt, and infection was carried out for 24 h.

For the production of control RNA (cRNA) and viral RNA (vRNA), A549 cells were either infected with

PR8 at an MOI of 5 for 8 h (vRNA) or mock infected with phosphate-buffered saline (PBS) (cRNA), and cells were lysed for RNA isolation. RNAs were then stored at -80°C until use. For stimulation with RNA, cells were transfected with cRNA/vRNA as described above for siRNA transfections. Cells were lysed at 3 hpt and processed for Western blot analyses.

Virus titration by standard plaque assays. Virus-containing supernatants were collected at the specified time points and stored at -80°C . Viral titers were assessed by standard plaque assays as described previously (32). Briefly, monolayers of MDCKII cells were infected with serial dilutions of IAV-containing supernatants for 30 min at 37°C to allow virus adsorption. The viral inoculum was subsequently aspirated and replaced with 2 ml of plaque medium (0.2% bovine serum albumin [BSA], 1 mM MgCl_2 , 0.9 mM CaCl_2 , 100 U/ml penicillin, 0.1 mg/ml streptomycin, 0.3% DEAE-dextran, and 1.5% NaHCO_3) supplemented with 0.6% agar (Oxoid). Plates were maintained at 37°C with 5% CO_2 for 3 days until manual counting of plaques. All results are expressed as PFU per milliliter.

RNA extraction, cDNA synthesis, and quantitative real-time PCR. A549 cells were infected with PR8 at an MOI of 5, and lysates were collected every 2 hpi until 8 h. RNA extraction was performed with a Monarch total RNA miniprep kit (New England BioLabs GmbH) according to the manufacturer's instructions. cDNA synthesis was performed with 1 μg of RNA and 0.5 μg of oligo(dT) primers, which were incubated for 5 min at 70°C , followed by 1 min at 4°C and 2 min at 37°C . The master mix (4 μl $5\times$ buffer, 2 μl [10 mM] deoxynucleoside triphosphate [dNTP], 0.5 μl Revert Aid H-minus reverse transcriptase) was added per sample as instructed by Thermo Fisher Scientific. The samples were then incubated for 1 h at 42°C , followed by 10 min at 70°C , and finally stored at -20°C until qRT-PCR assays. qRT-PCR was performed with 4 μl Brilliant III Ultra-Fast SYBR QPCR as instructed by the manufacturer (Agilent Santa Clara). All primers for the quantification of either the expression of viral mRNAs/cRNAs or antiviral responses are described below.

Primers for analyses of viral mRNAs are as follows: matrix protein 1 (M1) sense primer 5'-TGCAA AAACATCTTCAAGTCTCTG-3' and antisense primer 5'-AGATGAGTCTTCTAACCAGGTCG-3', polymerase basic protein 1 (PB1) sense primer 5'-CATACAGAAGACCAGTCGGGAT-3' and antisense primer 5'-GTCT GAGCTCTTCAATGGTGA-3', NS sense primer 5'-GAGGACTTGAATGGAATGATAACA-3' and antisense primer 5'-GTCTCAATTCTTCAATCAATCAACCATC-3', housekeeping gene GAPDH (glyceraldehyde-3-phosphate dehydrogenase) sense primer 5'-GCAAATTCATGGCACCGT-3' and antisense primer 5'-GCCCC ACTTGATTGGAGG-3', and SPAG9 sense primer 5'-GCTTTTGATCGCAATACAGAATCTC-3' and antisense primer 5'-AACTTCCGACCCATTCTAGT-3'.

Primers used for analyses of antiviral responses are as follows: IFN- β sense primer 5'-GCGCTC AGTTTCGGAGGTAACCTGT-3' and antisense primer 5'-GGCCATGACCAAGTGTCTCTCC-3', MxA sense primer 5'-GAAGGGCAACTCTGACAGT-3' and antisense primer 5'-GTTCCGAAGTGGACATCGCA-3', IP10 sense primer 5'-GGAACCTCCAGTCTCAGACCA-3' and antisense primer 5'-AGACATCTCTTCTACCCCTT C-3', and OAS1 sense primer 5'-CTGGCCAGGTGGAAGGAG-3' and antisense primer 5'-AGTACCTCGGAA GCACCTT-3'.

Strand-specific quantitative real-time PCR. The protocol and primers for cDNA synthesis and qRT-PCR were used as described previously (33). Briefly, 250 ng of RNA diluted in a total volume of 3.5 μl was incubated with 0.5 μl oligo(dT) and viral strand-specific primers for vRNA, cRNA, and mRNA. Samples were then incubated for 10 min at 65°C , 5 min at 4°C , and 5 min at 60°C before the addition of preheated master mix (4 μl first-strand buffer [$5\times$], 1 μl dithiothreitol [DTT], 1 μl [10 mM] dNTP, 0.5 μl Revert Aid Premium RT [Maxima], and 8 μl double-distilled water [ddH_2O]) according to the manufacturer's instructions (Thermo Fisher). Next, samples were incubated for 1 h at 60°C followed by 5 min at 85°C before storage at -20°C until qRT-PCR analyses. qRT-PCR was performed as explained above.

Western blot analysis. Cells were collected with radioimmunoprecipitation assay (RIPA) lysis buffer supplemented with protease and phosphatase inhibitors every 2 h after infection until 8 hpi and kept at -20°C . Samples were centrifuged, and relative protein amounts were determined by a Bradford assay (protein assay dye reagent concentrate; Bio-Rad). Subsequently, samples were diluted 5:1 in Laemmli buffer, separated by SDS-PAGE, and blotted using nitrocellulose membranes. Samples were analyzed for the expression of the viral proteins PB1, NS1, and M1 (Genetex) or cellular proteins such as tubulin, JIP4, p38, or p-p38 MAPK T180/Y182 (Cell Signaling Technology); pJNK pT183/pY185 (BD Bioscience); and JNK (Cell Signaling Technology).

Viral polymerase activity. Viral polymerase activity was measured in a minigenome assay as described previously (29). Briefly, Vero cells were transfected with a plasmid mixture of bidirectional pHW2000 vectors encoding the influenza A virus polymerase subunits PB1, polymerase basic protein 2 (PB2), polymerase acidic protein (PA) (200 ng each), and nucleoprotein (NP) (400 ng) as well as a polymerase I-driven expression plasmid (25 ng) expressing an influenza virus-like RNA coding for the reporter protein firefly luciferase (vRNA-luciferase) and a plasmid coding for renilla luciferase (25 ng) used for the normalization of transfection efficiencies. JIP4 (3 μg) was overexpressed together with the above-described plasmids. An EV (3 μg) was used as a positive control. As a negative control, the PB1 plasmid was excluded from the mix. Medium was exchanged for DMEM-10% FCS at 4 hpt, and cells were collected after 24 h for measurements of luciferase activity by a dual-luciferase assay (Promega). Relative light units (RLU) were normalized to the respective renilla activities and are expressed as percentages over the positive control.

The dose dependency of viral polymerase activity was measured in a similar approach with the same amounts of PB1, PB2, PA, and NP together with a polymerase I-driven expression plasmid (100 ng) that expresses an influenza virus-like RNA coding for the reporter protein firefly luciferase (vRNA-luciferase). JIP4 (0.1 to 3 μg) was overexpressed together with the above-described plasmids, and a GST expression

vector (pEBG) (0.1 to 3 μ g) was used as a positive control. RLU were normalized to the total protein amount and are expressed as percentages over the respective pEBG controls.

The effects of JIP4 knockdown on viral polymerase activity were assessed by transfection of a plasmid mixture of bidirectional pHW2000 vectors encoding PB1, PB2, PA, and NP in combination with the above-mentioned polymerase I-driven expression plasmid encoding firefly luciferase 48 h after siRNA transfection by using TransIT-LT1 (Mirus) according to the manufacturer's instructions. Viral polymerase activity was determined 24 h after DNA transfection. RLU were normalized to the total protein amount and are expressed as percentages over the siRNA control (siCNT).

Immunofluorescence. A549 cells seeded onto coverslips were transfected with the siRNA control or siRNA targeting JIP4 mRNA as described above. At 48 hpt, cells were infected with PR8 at an MOI of 20. For synchronization of infection, cells were maintained at 4°C for 1 h, followed by medium exchange and incubation at 37°C. At 3 hpi, cells were fixed with methanol for 10 min and maintained at 4°C in PBS. Blocking was performed with a 3% BSA–PBS solution for 90 min on a shaker. Thirty microliters of a primary antibody mix consisting of mouse anti-NP (catalog number MCA400; Bio-Rad) and rabbit anti-JIP4 (Cell Signaling Technology) diluted in 3% BSA was added, and the mixture was incubated for 1 h. Following three consecutive PBS washes, secondary antibodies (goat anti-rabbit IgG Alexa Fluor 488 from Invitrogen and goat anti-mouse Alexa Fluor 647 from Invitrogen) were added and incubated for 30 min, protected from light. After three additional PBS washes, nuclei were stained with 4',6-diamidino-2-phenylindole (DAPI) (Thermo Fisher) for 15 min, protected from light. Coverslips were then washed with PBS and mounted for microscopy analyses. Pictures were taken with a laser scanning microscope (LSM 780; Zeiss, Oberkochen, Germany) equipped with a Plan-Apochromat 63 \times (numerical aperture [NA], 1.4) oil immersion objective (Zeiss). All images were analyzed with the ImageJ program.

ACKNOWLEDGMENTS

We thank Saskia Hinse and Felicia Ye Wen Hwa for excellent technical assistance.

This work was supported by the German Research Foundation (DFG) (grants Lu477/23, BO5122/1-1, RTG 2220 A1, and SFB1009 TPB02), the Interdisciplinary Centre for Clinical Research (IZKF) (Lud2/017/13), and CAPES with a PDSE scholarship. The funders had no role in study design, data collection and interpretation, or the decision to submit the work for publication.

REFERENCES

- Dong G, Peng C, Luo J, Wang C, Han L, Wu B, Ji G, He H. 2015. Adamantane-resistant influenza A viruses in the world (1902–2013): frequency and distribution of M2 gene mutations. *PLoS One* 10:e0119115. <https://doi.org/10.1371/journal.pone.0119115>.
- Hayden FG, de Jong MD. 2011. Emerging influenza antiviral resistance threats. *J Infect Dis* 203:6–10. <https://doi.org/10.1093/infdis/jiq012>.
- Laure M, Hamza H, Koch-Heier J, Quernheim M, Müller C, Schreiber A, Müller G, Pleschka S, Ludwig S, Planz O. 2020. Antiviral efficacy against influenza virus and pharmacokinetic analysis of a novel MEK-inhibitor, ATR-002, in cell culture and in the mouse model. *Antiviral Res* 178:104806. <https://doi.org/10.1016/j.antiviral.2020.104806>.
- Nacken W, Ehrhardt C, Ludwig S. 2012. Small molecule inhibitors of the c-Jun N-terminal kinase (JNK) possess antiviral activity against highly pathogenic avian and human pandemic influenza A viruses. *Biol Chem* 393:525–534. <https://doi.org/10.1515/hsz-2011-0270>.
- Ludwig S, Ehrhardt C, Neumeier ER, Kracht M, Rapp UR, Pleschka S. 2001. Influenza virus-induced AP-1-dependent gene expression requires activation of the JNK signaling pathway. *J Biol Chem* 276:10990–10998. <https://doi.org/10.1074/jbc.M009902200>.
- Börgeling Y, Schmolke M, Viemann D, Nordhoff C, Roth J, Ludwig S. 2014. Inhibition of p38 mitogen-activated protein kinase impairs influenza virus-induced primary and secondary host gene responses and protects mice from lethal H5N1 infection. *J Biol Chem* 289:13–27. <https://doi.org/10.1074/jbc.M113.469239>.
- Kelkar N, Standen CL, Davis RJ. 2005. Role of the JIP4 scaffold protein in the regulation of mitogen-activated protein kinase signaling pathways. *Mol Cell Biol* 25:2733–2743. <https://doi.org/10.1128/MCB.25.7.2733-2743.2005>.
- Pinder A, Loo D, Harrington B, Oakes V, Hill MM, Gabrielli B. 2015. JIP4 is a PLK1 binding protein that regulates p38MAPK activity in G2 phase. *Cell Signal* 27:2296–2303. <https://doi.org/10.1016/j.cellsig.2015.08.009>.
- Marchesin V, Castro-Castro A, Lodillinsky C, Castagnino A, Cyrta J, Bonsang-Kitzys H, Fuhrmann L, Irondelle M, Infante E, Montagnac G, Reyal F, Vincent-Salomon A, Chavier P. 2015. ARF6-JIP3/4 regulate endosomal tubules for MT1-MMP exocytosis in cancer invasion. *J Cell Biol* 211:339–358. <https://doi.org/10.1083/jcb.201506002>.
- Killip MJ, Fodor E, Randall RE. 2015. Influenza virus activation of the interferon system. *Virus Res* 209:11–22. <https://doi.org/10.1016/j.virusres.2015.02.003>.
- Shim JM, Kim J, Tenson T, Min J-Y, Kainov DE. 2017. Influenza virus infection, interferon response, viral counter-response, and apoptosis. *Viruses* 9:223. <https://doi.org/10.3390/v9080223>.
- Kueck T, Bloyet L-M, Cassella E, Zang T, Schmidt F, Brusica V, Tekes G, Pornillos O, Whelan SPJ, Bieniasz PD, Pfeiffer JK. 2019. Vesicular stomatitis virus transcription is inhibited by TRIM69 in the interferon-induced antiviral state. *J Virol* 93:e01372–19. <https://doi.org/10.1128/JVI.01372-19>.
- Banerjee I, Miyake Y, Nobs SP, Schneider C, Horvath P, Kopf M, Matthias P, Helenius A, Yamauchi Y. 2014. Influenza A virus uses the aggresome processing machinery for host cell entry. *Science* 346:473–477. <https://doi.org/10.1126/science.1257037>.
- Fodor E. 2013. The RNA polymerase of influenza A virus: mechanisms of viral transcription and replication. *Acta Virol* 57:113–122. https://doi.org/10.4149/av_2013_02_113.
- Yasuda J, Whitmarsh AJ, Cavanagh J, Sharma M, Davis RJ. 1999. The JIP group of mitogen-activated protein kinase scaffold proteins. *Mol Cell Biol* 19:7245–7254. <https://doi.org/10.1128/MCB.19.10.7245>.
- Nacken W, Wixler V, Ehrhardt C, Ludwig S. 2017. Influenza A virus NS1 protein-induced JNK activation and apoptosis are not functionally linked. *Cell Microbiol* 19:e12721. <https://doi.org/10.1111/cmi.12721>.
- Hrincius ER, Wixler V, Wolff T, Wagner R, Ludwig S, Ehrhardt C. 2010. CRK adaptor protein expression is required for efficient replication of avian influenza A viruses and controls JNK-mediated apoptotic responses. *Cell Microbiol* 12:831–843. <https://doi.org/10.1111/j.1462-5822.2010.01436.x>.
- Ludwig S, Wang X, Ehrhardt C, Zheng H, Donelan N, Planz O, Pleschka S, García-Sastre A, Heins G, Wolff T. 2002. The influenza A virus NS1 protein inhibits activation of Jun N-terminal kinase and AP-1 transcription factors. *J Virol* 76:11166–11171. <https://doi.org/10.1128/jvi.76.21.11166-11171.2002>.
- Bonet-Ponce L, Beilina A, Williamson CD, Lindberg E, Kluss JH, Saez-Atienzar S, Landeck N, Kumaran R, Mamais A, Bleck CKE, Li Y, Cookson MR. 2020. LRRK2 mediates tubulation and vesicle sorting from lysosomes. *Sci Adv* 6:eabb2454. <https://doi.org/10.1126/sciadv.abb2454>.

20. Pan C, Olsen JV, Daub H, Mann M. 2009. Global effects of kinase inhibitors on signaling networks revealed by quantitative phosphoproteomics. *Mol Cell Proteomics* 8:2796–2808. <https://doi.org/10.1074/mcp.M900285-MCP200>.
21. Parker R, Vella LJ, Xavier D, Amirkhani A, Parker J, Cebon J, Molloy MP. 2015. Phosphoproteomic analysis of cell-based resistance to BRAF inhibitor therapy in melanoma. *Front Oncol* 5:95. <https://doi.org/10.3389/fonc.2015.00095>.
22. Holzberg M, Boergeling Y, Schröder T, Ludwig S, Ehrhardt C. 2017. Vemurafenib limits influenza A virus propagation by targeting multiple signaling pathways. *Front Microbiol* 8:2426. <https://doi.org/10.3389/fmicb.2017.02426>.
23. Ludwig S. 2009. Targeting cell signalling pathways to fight the flu: towards a paradigm change in anti-influenza therapy. *J Antimicrob Chemother* 64:1–4. <https://doi.org/10.1093/jac/dkp161>.
24. Schröder T, Dudek SE, Schreiber A, Ehrhardt C, Planz O, Ludwig S. 2018. The clinically approved MEK inhibitor trametinib efficiently blocks influenza A virus propagation and cytokine expression. *Antiviral Res* 157: 80–92. <https://doi.org/10.1016/j.antiviral.2018.07.006>.
25. Marjuki H, Gornitzky A, Marathe BM, Ilyushina NA, Aldridge JR, Desai G, Webby RJ, Webster RG. 2011. Influenza A virus-induced early activation of ERK and PI3K mediates V-ATPase-dependent intracellular pH change required for fusion. *Cell Microbiol* 13:587–601. <https://doi.org/10.1111/j.1462-5822.2010.01556.x>.
26. Schreiber A, Boff L, Anhlan D, Krischuns T, Brunotte L, Schuberth C, Wedlich-Söldner R, Drexler H, Ludwig S. 2020. Dissecting the mechanism of signaling-triggered nuclear export of newly synthesized influenza virus ribonucleoprotein complexes. *Proc Natl Acad Sci U S A* 117:16557–16566. <https://doi.org/10.1073/pnas.2002828117>.
27. Mazur I, Wurzer WJ, Ehrhardt C, Pleschka S, Puthavathana P, Silberzahn T, Wolff T, Planz O, Ludwig S. 2007. Acetylsalicylic acid (ASA) blocks influenza virus propagation via its NF-kappaB-inhibiting activity. *Cell Microbiol* 9:1683–1694. <https://doi.org/10.1111/j.1462-5822.2007.00902.x>.
28. Wurzer WJ, Ehrhardt C, Pleschka S, Berberich-Siebelt F, Wolff T, Walczak H, Planz O, Ludwig S. 2004. NF-kappaB-dependent induction of tumor necrosis factor-related apoptosis-inducing ligand (TRAIL) and Fas/FasL is crucial for efficient influenza virus propagation. *J Biol Chem* 279: 30931–30937. <https://doi.org/10.1074/jbc.M403258200>.
29. Mänz B, Brunotte L, Reuther P, Schwemmler M. 2012. Adaptive mutations in NEP compensate for defective H5N1 RNA replication in cultured human cells. *Nat Commun* 3:802. <https://doi.org/10.1038/ncomms1804>.
30. Carpy A, Patel A, Tay YD, Hagan IM, Macek B. 2015. Nic1 inactivation enables stable isotope labeling with ¹³C615N4-arginine in *Schizosaccharomyces pombe*. *Mol Cell Proteomics* 14:243–250. <https://doi.org/10.1074/mcp.O114.045302>.
31. Macek J, Ptáček P, Klíma J. 2009. Determination of tolterodine and its 5-hydroxymethyl metabolite in human plasma by hydrophilic interaction liquid chromatography-tandem mass spectrometry. *J Chromatogr B Analyt Technol Biomed Life Sci* 877:968–974. <https://doi.org/10.1016/j.jchromb.2009.02.036>.
32. Seyer R, Hrincius ER, Ritzel D, Abt M, Mellmann A, Marjuki H, Kühn J, Wolff T, Ludwig S, Ehrhardt C. 2012. Synergistic adaptive mutations in the hemagglutinin and polymerase acidic protein lead to increased virulence of pandemic 2009 H1N1 influenza A virus in mice. *J Infect Dis* 205:262–271. <https://doi.org/10.1093/infdis/jir716>.
33. Kawakami E, Watanabe T, Fujii K, Goto H, Watanabe S, Noda T, Kawaoka Y. 2011. Strand-specific real-time RT-PCR for distinguishing influenza vRNA, cRNA, and mRNA. *J Virol Methods* 173:1–6. <https://doi.org/10.1016/j.jviromet.2010.12.014>.